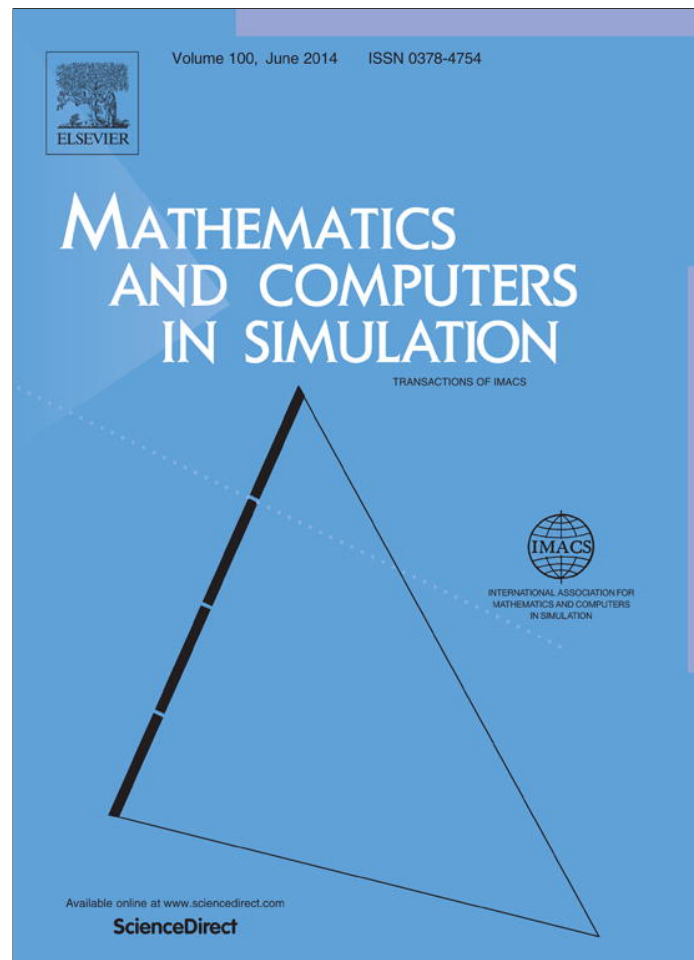


Provided for non-commercial research and education use.
Not for reproduction, distribution or commercial use.



This article appeared in a journal published by Elsevier. The attached copy is furnished to the author for internal non-commercial research and education use, including for instruction at the authors institution and sharing with colleagues.

Other uses, including reproduction and distribution, or selling or licensing copies, or posting to personal, institutional or third party websites are prohibited.

In most cases authors are permitted to post their version of the article (e.g. in Word or Tex form) to their personal website or institutional repository. Authors requiring further information regarding Elsevier's archiving and manuscript policies are encouraged to visit:

<http://www.elsevier.com/authorsrights>



ELSEVIER



CrossMark

Available online at www.sciencedirect.com

ScienceDirect

Mathematics and Computers in Simulation 100 (2014) 41–53


 MATHEMATICS
AND
COMPUTERS
IN SIMULATION

www.elsevier.com/locate/matcom

Original Article

IMSP schemes for spatially explicit models of cyclic populations and metapopulation dynamics

 Fasma Diele^{a,*}, Carmela Marangi^a, Stefania Ragni^{a,b}
^a *Istituto per le Applicazioni del Calcolo M. Picone, CNR, Via Amendola 122/D, 70126 Bari, Italy*
^b *Dipartimento di Scienze Economiche e Aziendali, Università di Sassari, Via Muroni 25, 07100 Sassari, Italy*

Received 15 March 2013; received in revised form 6 November 2013; accepted 13 January 2014

Available online 3 March 2014

Abstract

We examine spatially explicit models described by reaction-diffusion partial differential equations for the study of predator–prey population dynamics. The numerical methods we propose are based on the coupling of a finite difference/element spatial discretization and a suitable partitioned Runge–Kutta scheme for the approximation in time. The RK scheme here implemented uses an implicit scheme for the stiff diffusive term and a partitioned RK symplectic scheme for the reaction term (IMSP scheme). We revisit some results provided in literature for the classical Lotka–Volterra system and the Rosenzweig–MacArthur model. We then extend the approach to metapopulation dynamics in order to numerically investigate the effect of migration through a corridor connecting two habitat patches. Moreover, we analyze the synchronization properties of subpopulation dynamics, when the migration occurs through corridors of variable size.

© 2014 IMACS. Published by Elsevier B.V. All rights reserved.

Keywords: Predator–prey dynamics; Runge–Kutta schemes; Poisson integrators

1. Introduction

The study of populations undergoing multi-year cycles has renewed the interest on non-linear dynamical systems characterized by spatio-temporal patterns formation. Critical fluctuations, oscillations, waves, chaos, are examples of complex phenomena that have been thoroughly researched in recent literature [26]. The easiest way to model the dynamics of cyclic populations, that leads to pattern formation, is through oscillatory reaction-diffusion equations. The solutions of such equations are sufficiently rich in their spatiotemporal dynamics to allow for the description of phenomena such as species invasion, species persistence, and biological chaos [22]. Moreover, spatially interacting populations are widely described in literature using metapopulation models where the reaction-diffusion equations are coupled via migration terms [11].

The numerical approximation of such models is a challenging aspect of the problem that deserves great attention. Following the approach of [10,12] we address the issue above by coupling difference schemes for the approximation in space to suitable schemes for the approximation in time, which allow us to mimic the properties of the dynamical

* Corresponding author. Tel.: +39 080 5929747; fax: +39 080 5929770.

E-mail addresses: f.diele@ba.iac.cnr.it (F. Diele), c.marangi@ba.iac.cnr.it (C. Marangi), s.ragni@ba.iac.cnr.it (S. Ragni).

Table 1
Reaction terms for the different predator–prey models.

Model	$H(u)$	$F(u)$	$G(u)$	$P(u, v)$
LV	r	cu	χcu	γ
RM	$r \left(1 - \frac{u}{k}\right)$	$\frac{cu}{l+u}$	$\frac{\chi cu}{l+u}$	γ
May	$r \left(1 - \frac{u}{k}\right)$	$\frac{cu}{l+u}$	s	$\frac{qv}{u}$
VT	$r \left(1 - \frac{u}{k}\right)$	$\frac{cu}{l+u}$	$\frac{\chi cu}{l+u}$	$\gamma + \frac{sqv}{u}$

systems within the limit of a spatially uniform process. Such schemes have been originally introduced in [7] and are here extended to account for a spatially explicit model in a metapopulation approach. The paper is organized as follows: in Section 2 the reaction-diffusion models for cyclic populations are briefly described and the proposed IMSP schemes are introduced. Results on the two most popular predator–prey models are illustrated. In Section 3 we describe how the IMSP schemes have been tailored on the spatially explicit metapopulation models. The results obtained on the Rosenzweig–MacArthur (RM) [25] model, when applied to a two-patch fragmented habitat connected via a corridor, are shown in Section 4. In the same section we briefly show the effect of the variable size of the corridor on the synchronization of the dynamics in the two patches as induced by migration through the corridor. Finally we draw our conclusions in Section 5.

2. IMSP Runge–Kutta methods for cyclic populations

Predator–prey spatially extended dynamics can be described by reaction-diffusion systems in the general form

$$\begin{aligned} \frac{\partial u}{\partial t} &= \epsilon^{(u)} \Delta u + g_u(u, v), \\ \frac{\partial v}{\partial t} &= \epsilon^{(v)} \Delta v + g_v(u, v), \end{aligned} \tag{1}$$

where the real valued functions $u = u(x, t)$ and $v = v(x, t)$ represent prey and predator densities at time $t \leq T$ in a bounded domain $\Omega \subset \mathbb{R}^M$ ($M \leq 3$) and Δ is the Laplace operator. The diffusivity coefficients $\epsilon^{(u)}$ and $\epsilon^{(v)}$ are supposed to be non negative, meaning that the dynamics may lose the dependence on spatial variables when both $\epsilon^{(u)}$ and $\epsilon^{(v)}$ assume zero value. Moreover, suitable initial conditions $u_0(x) = u(x, 0)$, $v_0(x) = v(x, 0)$ and zero-flux boundary ones are provided.

We focus our interest on cyclic populations: as was done in [26] we assume that the local dynamics is modelled by the spatially uniform equations

$$\begin{aligned} \frac{du}{dt} &= g_u(u, v), \\ \frac{dv}{dt} &= g_v(u, v). \end{aligned}$$

which have a periodic solution (center or limit cycle), that oscillates around an unstable coexistence steady state. In general, reaction terms for cyclic population dynamics (see for example [28]) are defined by

$$\begin{aligned} g_u(u, v) &= u H(u) - v F(u) \\ g_v(u, v) &= v G(u) - v P(u, v) \end{aligned} \tag{2}$$

where function $H(u)$ is the intrinsic growth rate of preys, $F(u)$ gives the functional response of preys to predators, $G(u)$ is the prey dependent growth rate of the predator and $P(u, v)$ represents the prey dependent functional response of predators to preys. These functions vary according to the model which is considered. Lotka–Volterra (LV) [24] system as well as its modifications such as the Rosenzweig–MacArthur (RM) [25], the May [20] and the variable territory (VT) [29] are the most widely used differential models considered in this framework. The reaction terms in the LV, RM, MAY and VT models are defined in different ways according to Table 1 (see [4] and [9]).

The spatiotemporal dynamics modelled by two-species predator–prey interactions, and described by reaction–diffusion systems, have attracted a lot of interest in the mathematical–ecological research community. We refer to paper [22], for an extensive reference list concerning this topics, as well as review paper [26], where the specific problem of generating periodic travelling waves in cyclic dynamics is addressed. Moreover, we refer to the large production of work by Garvie (for instance, [10–12]) that focuses on numerical approaches for achieving stable and accurate approximated solutions.

Inspired by the results in [10] and [12], we shift our attention to the numerical treatment of this kind of systems. In particular, we propose a different scheme for approximating the time evolution, designed to provide more stable results and to reproduce the same qualitative behaviour of the theoretical solution. We start by introducing vector $\mathbf{y} = [u, v]^T$, then system (1) can be written as the following semi-linear parabolic equation:

$$\frac{\partial \mathbf{y}}{\partial t} = L\mathbf{y} + g(\mathbf{y}), \tag{3}$$

where $L = \text{diag}(\epsilon^{(u)} \Delta, \epsilon^{(v)} \Delta)$ is a linear partial differential operator and $g(\mathbf{y}) = [g_u(u, v), g_v(u, v)]^T$.

In order to perform a spatial discretization of the problem, we consider a grid $\Omega_h \subset \Omega$ with mesh width $h > 0$. The model can be discretized with respect to the spatial variable by means of classical techniques, such as finite elements or finite differences. The resulting problem consists of an ordinary differential system

$$\frac{d y}{d t} = L_h y + g_h(y), \tag{4}$$

whose solution $y(t) = [u_h(t), v_h(t)]^T$ represents an approximation on the given mesh Ω_h . We remark that $L_h = \text{diag}(\epsilon^{(u)} \Delta_h, \epsilon^{(v)} \Delta_h)$ is a discrete operator approximating L and g_h is the restriction of g onto Ω_h itself.

One of the most popular approaches for integrating (4) is to apply an implicit–explicit (IMEX) Runge–Kutta method: indeed, it is possible to introduce two variables y_1 and y_2 such that $y = y_1 + y_2$ and to consider the equivalent system

$$\frac{d y_1}{d t} = L_h(y_1 + y_2), \quad \frac{d y_2}{d t} = g_h(y_1 + y_2),$$

which can be handled by a partitioned Runge–Kutta scheme consisting of a diagonally implicit method joint with an explicit one (see [18]). This approach is motivated by the fact that the stiff term L_h has to be suitably approximated by an implicit scheme, while an explicit method is used to discretize the non-stiff (or mildly stiff) term g_h . For instance, the Euler IMEX Runge–Kutta scheme is defined as

$$y_h^{n+1} = y_h^n + h_T L_h(y_h^{n+1}) + h_T g_h(y_h^n),$$

where y_h^n approximates the solution $y_h(t_n) = [u_h(t_n), v_h(t_n)]^T$ at any discrete time $t_n = n h_T$, with uniform time step length h_T .

Recently, in [7] the authors have proposed to split the problem in order to have $y = y_1 + y_2 + y_3$ and

$$\begin{aligned} \frac{d y_1}{d t} &= L_h(y_1 + y_2 + y_3), \\ \frac{d y_2}{d t} &= g_h^{(u)}(y_1 + y_2 + y_3), \\ \frac{d y_3}{d t} &= g_h^{(v)}(y_1 + y_2 + y_3), \end{aligned}$$

with $g_h = g_h^{(u)} + g_h^{(v)}$, $g_h^{(u)} = [g_u(u_h, v_h), \mathbf{0}]^T$, $g_h^{(v)} = [\mathbf{0}, g_v(u_h, v_h)]^T$. A partitioned Runge–Kutta scheme is employed to solve the above model: the dynamics of y_1 is approximated by a diagonally implicit method, whereas the evolution of y_2 and y_3 variables is described by a partitioned symplectic Runge–Kutta method defined as

$$\left| \begin{array}{cccccc} 0 & & & & & \\ \beta_1 & \alpha_1 & & & & \\ \vdots & \vdots & & \ddots & & \\ \beta_1 & \alpha_1 & \dots & \dots & 0 & \\ \beta_1 & \alpha_1 & \dots & \dots & \beta_s & \alpha_s \\ \hline \beta_1 & \alpha_1 & \dots & \dots & \beta_s & \alpha_s \end{array} \right| \quad \left| \begin{array}{cccccc} \beta_1 & & & & & \\ \beta_1 & 0 & & & & \\ \vdots & \vdots & & \ddots & & \\ \beta_1 & \alpha_1 & \dots & \dots & \beta_s & \\ \beta_1 & \alpha_1 & \dots & \dots & \beta_s & 0 \\ \hline \beta_1 & \alpha_1 & \dots & \dots & \beta_s & \alpha_s \end{array} \right| \tag{5}$$

This choice is motivated by specific features that characterize the problem (see [19]). In particular it is known that, when functions g_u and g_v are defined according to the Lotka–Volterra model, then the problem becomes spatially homogeneous as $t \rightarrow \infty$ and it is controlled by the classical Lotka–Volterra ODE

$$\begin{aligned} \frac{du}{dt} &= r u - c u v, \\ \frac{dv}{dt} &= \chi c v u - \gamma v, \end{aligned}$$

where r, c, χ, γ are strictly positive constants. It can be proved that the quantity $H(\mathbf{y}) = r \ln(v) - cv + \gamma \ln(u) - \chi c u$ represents an invariant for this model, which can be given in the following Poisson form

$$\frac{d\mathbf{y}}{dt} = B(\mathbf{y}) \nabla H(\mathbf{y}),$$

where we define

$$B(\mathbf{y}) = \begin{pmatrix} 0 & u v \\ -u v & 0 \end{pmatrix}.$$

In this respect, we remark that Poisson integrators related to the structure of $B(\mathbf{y})$ have to be employed in order to produce an excellent long time behaviour with respect to the approximation of the invariant $H(\mathbf{y})$. In [6] it is shown that the partitioned Runge–Kutta scheme (5) is given by the composition of a symplectic Euler scheme with its adjoint. Since both these methods represent Poisson integrators, then the scheme (5) is a Poisson integrator itself, for the Lotka–Volterra system¹ (for more details see [13]).

We set $s = 1$ and apply the following two-stage schemes

$$\left| \begin{array}{cc} 0 & 0 \\ \alpha & \beta \end{array} \right| \quad \left| \begin{array}{cc} 0 & 0 \\ \beta & \alpha \end{array} \right| \quad \left| \begin{array}{cc} \beta & 0 \\ \beta & 0 \end{array} \right| \quad \left| \begin{array}{cc} \beta & 0 \\ \beta & \alpha \end{array} \right| \tag{6}$$

where the first tableau represents the diagonally implicit method to be used for approximating the dynamics of y_1 , and the remaining tableaus are related to the partitioned symplectic Runge–Kutta scheme defined in (5) (here $\beta = \beta_1$, $\alpha = \alpha_1$, the subscript is omitted to simplify the notation) in order to discretize y_2 and y_3 . The overall method defined by (6) is again a partitioned Runge–Kutta scheme and it is given by

$$\begin{aligned} Y_h^{n,1} &= y_h^n + h_T \beta g_h^{(v)}(Y_h^{n,1}), \\ Y_h^{n,2} &= Y_h^{n,1} + h_T \alpha L_h Y_h^{n,1} + h_T \beta g_h^{(u)}(Y_h^{n,1}) + h_T \beta L_h Y_h^{n,2} + h_T \alpha g_h^{(u)}(Y_h^{n,2}), \\ y_h^{n+1} &= Y_h^{n,2} + h_T \alpha g_h^{(v)}(Y_h^{n,2}). \end{aligned} \tag{7}$$

¹ We remark that, in [7], the authors have addressed the good performance of the IMSP methods with respect to the symplecticity property of the partitioned Runge–Kutta method proposed therein. Here we point out that such good results are due to the fact that the method is a Poisson integrator for the ODE Lotka–Volterra system.

Let us remark that for $\beta = 1$ and $\alpha = 0$ this scheme is featured by a first order approximation; when $\beta = \alpha = 1/2$, we get a second order accurate method.

Moreover, under the assumption that diffusivity coefficients ϵ_u and ϵ_v nullify, the first order scheme represents a symplectic Euler scheme which handles the variable u_h in an explicit way and the variable v_h in an implicit one. The second order approximation reduces to the classical Störmer–Verlet scheme when it is written as a partitioned Runge–Kutta method exploiting the trapezoidal rule in order to approximate the stiff diffusive term.

A better choice may turn out to be the selection of methods with the stronger stability feature of L-stability (see [1]). Accordingly, we consider the following method which is composed by a singular diagonally implicit Runge–Kutta scheme coupled with the second order symmetric symplectic partitioned one (see [21]):

$$\begin{array}{c|ccc|ccc|ccc}
 \beta & 0 & 0 & 0 & 0 & 0 & 0 & 0 & \beta & 0 & 0 & 0 \\
 0 & \beta & 0 & 0 & \beta & \alpha & 0 & 0 & \beta & 0 & 0 & 0 \\
 0 & 0 & \beta & 0 & \beta & \alpha & 0 & 0 & \beta & \alpha & \alpha & 0 \\
 \beta & \alpha & \alpha & \beta & \beta & \alpha & \alpha & \beta & \beta & \alpha & \alpha & 0 \\
 \hline
 \beta & \alpha & \alpha & \beta & \beta & \alpha & \alpha & \beta & \beta & \alpha & \alpha & \beta
 \end{array} \tag{8}$$

where we set $\beta = \tilde{\beta}$ and $\alpha = 1/2 - \tilde{\beta}$. It is known that, assuming $\tilde{\beta} = 1 - \sqrt{2}/2$, the previous method (8) is globally second order accurate and it is L-stable concerning the diffusive term.

An application of the previous first order schemes and a comparison with the Euler IMEX scheme for the solution of a two-dimensional dynamics with a LV reaction term is shown in Fig. 1. We provide the phase portrait of prey versus predator densities in the center $x_c = [10, 10]$ of a domain $\Omega = [0, 20] \times [0, 20]$. The solution follows a closed trajectory which is well reproduced by the IMSP scheme whereas an outward spiraling solution results from the application of the IMEX scheme. As a further test, we approximate the chaotic dynamics of the two-dimensional model (1) where the reaction term is defined by the Rosenzweig–MacArthur model. In particular, we consider the same parameters exploited in [10] and [22]. The problem can be viewed as a model for marine plankton dynamics in a dimensionless form; in correspondence with different initial conditions for the state variables, both [10] and [22] numerically show that the system is affected by spatio-temporal chaos, in the sense that spiral patterns appear together with irregular patches that spread over the whole domain. It is remarkable that, in the numerical tests performed in [10], the spiral patterns found in [22] disappear when the time discretization is refined. Thus the authors argue that some spiral patterns are probably a numerical artifact which can be removed by improving the numerical solution in stability and accuracy. This hypothesis is confirmed by our numerical tests which show that the spiraling pattern resulting from the application of the classical IMEX scheme disappears in the simulations performed by IMSP algorithms (see Figs. 2 and 3).

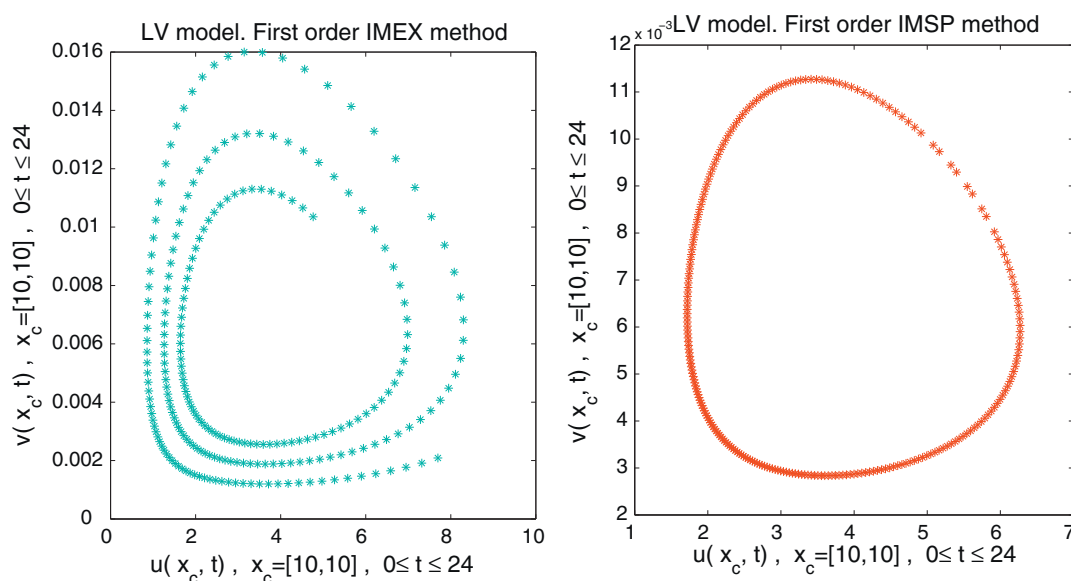


Fig. 1. Approximate solutions at the center of the domain $\Omega = [0, 20] \times [0, 20]$ in the time interval $[0, 24]$. Model parameters: $\epsilon^{(u)} = 1.5$, $\epsilon^{(v)} = 2$, $r = 0.75$, $\chi = 1.97 \times 10^{-3}$, $\gamma = 0.85$, $c = 122$. $u_0 = 5$, $v_0 = 0.01$ (see [28]). Method parameters: $h = h_T = 0.1$.

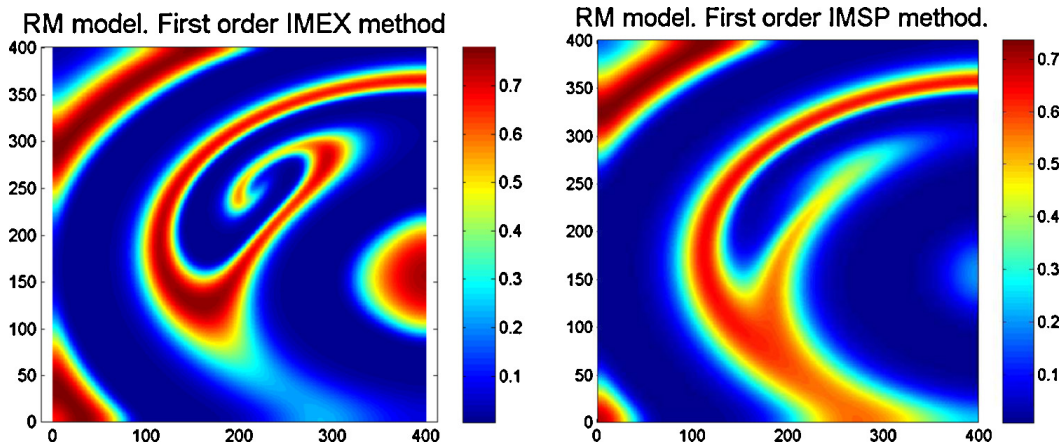


Fig. 2. First order approximations at $t=120$ in $\Omega=[0, 400] \times [0, 400]$ with $h=1$ and $h_T=1/3$. Model parameters: $\epsilon^{(u)}=1$, $\epsilon^{(v)}=1$, $r=k=c=1$, $\chi=2$, $\gamma=0.6$, $l=0.4$. Initial values: $u_0=6/35 - 2 \times 10^{-7} (X-180)(X-720) - 6 \times 10^{-7} (Y-90)(Y-210)$, $v_0=116/245 - 3 \times 10^{-5} (X-450) - 6 \times 10^{-5} (Y-135)$ (see [10]).

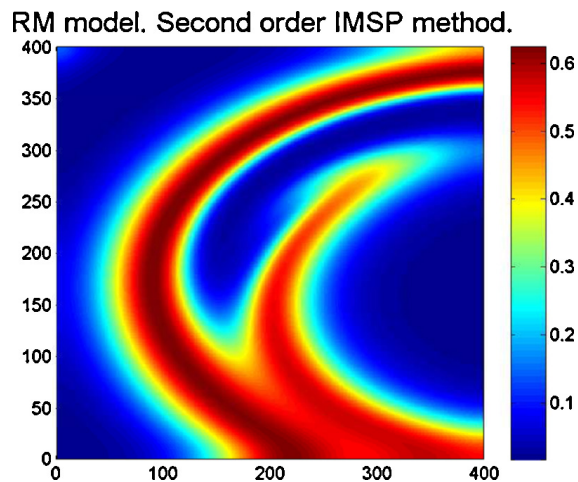


Fig. 3. Second order approximation at $t=120$ in $\Omega=[0, 400] \times [0, 400]$ with $h=1$ and $h_T=1/3$. Model parameters: $\epsilon^{(u)}=1$, $\epsilon^{(v)}=1$, $r=k=c=1$, $\chi=2$, $\gamma=0.6$, $l=0.4$. Initial values: $u_0=6/35 - 2 \times 10^{-7} (X-180)(X-720) - 6 \times 10^{-7} (Y-90)(Y-210)$, $v_0=116/245 - 3 \times 10^{-5} (X-450) - 6 \times 10^{-5} (Y-135)$ (see [10]).

3. IMSP schemes for spatially explicit cyclic metapopulation dynamics

A simple formalism to describe spatially interacting populations is provided by the so-called metapopulation models. A metapopulation consists of a set of local populations living in patches, which are connected through migration. Metapopulation dynamics, i.e. the dynamics of a “population of populations” (see [16]), represents an effective tool for investigating the dispersal of some species in fragmented habitat. We introduce a simplistic and convenient spatially explicit metapopulation model as composed of M patches where the movement of each predator–prey subpopulation is modelled by a reaction-diffusion problem as the one described in (1). More precisely, we consider the following differential system

$$\begin{aligned} \frac{\partial u_i}{\partial t} &= \epsilon^{(u_i)} \Delta u_i + g_u(u_i, v_i) + \sum_{j=1}^M D_{i,j}^{(u)}(x)(u_j - u_i), \\ \frac{\partial v_i}{\partial t} &= \epsilon^{(v_i)} \Delta v_i + g_v(u_i, v_i) + \sum_{j=1}^M D_{i,j}^{(v)}(x)(v_j - v_i), \end{aligned} \tag{9}$$

for $i=1, \dots, M$, where $u_i = u_i(x, t)$ and $v_i = v_i(x, t)$ represent the concentrations of prey and predator population at each time t and position x within the patch $\Omega_i \subset \mathbf{R}^m$, ($1 \leq m \leq 3$), then $\Delta = \sum_{j=1}^m (\partial^2 / \partial x_j^2)$ is the Laplacian operator, $\epsilon_i^{(u)}$,

$\epsilon_i^{(v)}$ are the diffusivity coefficients for the prey and the predator in every patch Ω_i . The matrices $D_{i,j}^{(u)}(x)$ and $D_{i,j}^{(v)}(x)$ are supposed symmetric and their entries represent the migration rates between patches Ω_i and Ω_j for preys and predators, respectively, at position x . We assume that migration occurs only at given positions, which correspond to the corridor entrances, and that each corridor has no physical length. By defining as $C_{i,j}$ the entrance of the corridor connecting Ω_i to Ω_j , we have that $C_{i,j} = C_{j,i}$ and $C_{i,j} \subset \Omega_i \cap \Omega_j$. Moreover, we suppose migration rates take constant values in each corridor, i.e. $D_{i,j}^{(u)}(x) = d_{i,j}^{(u)}$ and $D_{i,j}^{(v)}(x) = d_{i,j}^{(v)}$ for every $x \in C_{i,j}$, with $d_{i,j}^{(u)}, d_{i,j}^{(v)} > 0$, otherwise $D_{i,j}^{(u)}(x) = D_{i,j}^{(v)}(x) = 0$. System (9) is completed by suitable initial conditions $u_i(x, 0) = u_{i,0}(x)$ and $v_i(x, 0) = v_{i,0}(x)$ for $x \in \Omega_i$, and homogeneous Neumann boundary conditions $\partial u_i(x, t) / \partial n_i = \partial v_i(x, t) / \partial n_i = 0$ for $(x, t) \in \partial \Omega_i \times \mathbf{R}^+$, where n_i is the outward normal vector to the boundary $\partial \Omega_i$, for $i = 1, \dots, M$. The choice of zero-flux boundary conditions means that the species cannot leave their patches, except via migration.

We are interested in applying IMSP methods described in Section 2 in order to solve model (9). With this aim, we remark that it can be written as in Eq. (3), where we set $\mathbf{y} = [u_1, \dots, u_M, v_1, \dots, v_M]^T$,

$$L = \begin{pmatrix} \epsilon^{(u_1)} \Delta & 0 & 0 & 0 & 0 & 0 \\ 0 & \ddots & 0 & 0 & 0 & 0 \\ 0 & 0 & \epsilon^{(u_M)} \Delta & 0 & 0 & 0 \\ 0 & 0 & 0 & \epsilon^{(v_1)} \Delta & 0 & 0 \\ 0 & 0 & 0 & 0 & \ddots & 0 \\ 0 & 0 & 0 & 0 & 0 & \epsilon^{(v_M)} \Delta \end{pmatrix},$$

and

$$g(\mathbf{y}) = \begin{pmatrix} g_u(u_1, v_1) + \sum_{j=1}^M D_{1,j}^{(u)}(x)(u_j - u_1) \\ \vdots \\ g_u(u_M, v_M) + \sum_{j=1}^M D_{M,j}^{(u)}(x)(u_j - u_M) \\ g_v(u_1, v_1) + \sum_{j=1}^M D_{1,j}^{(v)}(x)(v_j - v_1) \\ \vdots \\ g_v(u_M, v_M) + \sum_{j=1}^M D_{M,j}^{(v)}(x)(v_j - v_M) \end{pmatrix}.$$

When a spatial discretization is performed, then the resulting problem consists of an ordinary differential equation as in (4) where the discrete operator is given by

$$L_h = \begin{pmatrix} \epsilon^{(u_1)} \Delta_h & 0 & 0 & 0 & 0 & 0 \\ 0 & \ddots & 0 & 0 & 0 & 0 \\ 0 & 0 & \epsilon^{(u_M)} \Delta_h & 0 & 0 & 0 \\ 0 & 0 & 0 & \epsilon^{(v_1)} \Delta_h & 0 & 0 \\ 0 & 0 & 0 & 0 & \ddots & 0 \\ 0 & 0 & 0 & 0 & 0 & \epsilon^{(v_M)} \Delta_h \end{pmatrix},$$

and the forcing term g is evaluated at each spatial node of the given mesh Ω_h .

We consider the splitting $g_h = g_h^{(u)} + g_h^{(v)}$ with

$$g_h^{(u)}(y_h) = \begin{pmatrix} g_u(u_{h,1}, v_{h,1}) + \sum_{j=1}^N \hat{D}_{1,j}^{(u)}(u_{h,j} - u_{h,1}) \\ \vdots \\ g_u(u_{h,M}, v_{h,M}) + \sum_{j=1}^M \hat{D}_{M,j}^{(u)}(u_{h,j} - u_{h,M}) \\ \mathbf{0}_M \end{pmatrix},$$

and

$$g_h^{(v)}(y_h) = \begin{pmatrix} \mathbf{0}_M \\ g_v(u_{h,1}, v_{h,1}) + \sum_{j=1}^M \hat{D}_{1,j}^{(v)}(v_{h,j} - v_{h,1}) \\ \vdots \\ g_v(u_{h,M}, v_{h,M}) + \sum_{j=1}^M \hat{D}_{M,j}^{(v)}(v_{h,j} - v_{h,M}) \end{pmatrix}$$

where $\hat{D}^{(u)}$ and $\hat{D}^{(v)}$ are the restrictions of matrices $D^{(u)}$ and $D^{(v)}$ onto Ω_h and $\mathbf{0}_M$ represents the null M -dimensional vector. The first order IMSP scheme (7) obtained for $\beta = 1$ and $\alpha = 0$ is given by the following formula

$$Y_h^{n,1} = y_h^n + h_T g_h^{(v)}(Y_h^{n,1}),$$

$$y_h^{n+1} = Y_h^{n,1} + h_T L_h y_h^{n+1} + h_T g_h^{(u)}(Y_h^{n,1}),$$

where y_h^n approximates $y_h(t_n) = [u_{h,1}(t_n), \dots, u_{h,M}(t_n), v_{h,1}(t_n), \dots, v_{h,M}(t_n)]^T$.

In terms of $u_{h,i}$ and $v_{h,i}$ the previous scheme requires the solution of the following system for the intermediate steps $V_{h,i}^n$

$$V_{h,i}^n - h_T V_{h,i}^n G(u_{h,i}^n) + h_T V_{h,i}^n P(u_{h,i}^n, V_{h,i}^n) - h_T \sum_{j=1}^M \hat{D}_{i,j}^{(v)}(V_{h,j}^n - V_{h,i}^n) = v_{h,i}^n, \tag{10}$$

the evaluation of

$$U_{h,i}^n = u_{h,i}^n + h_T u_{h,i}^n H(u_{h,i}^n) - h_T V_{h,i}^n F(u_{h,i}^n) + h_T \sum_{j=1}^M \hat{D}_{i,j}^{(u)}(u_{h,j}^n - u_{h,i}^n),$$

and the solution of the two uncoupled M -dimensional linear systems

$$u_{h,i}^{n+1} - h_T \epsilon^{(u_i)} \Delta_h u_{h,i}^{n+1} = U_{h,i}^n,$$

$$v_{h,i}^{n+1} - h_T \epsilon^{(v_i)} \Delta_h v_{h,i}^{n+1} = V_{h,i}^n.$$

It is simple to verify that, when diffusive coefficients $\epsilon^{(u_i)}$ and $\epsilon^{(v_i)}$ nullify, the previous scheme represents the classical partitioned symplectic Euler method. From a computational point of view, when the LV and RM models are considered, then $P(u, v) = \gamma$ and the nonlinear equations in (10) reduce to a linear system with respect to the unknown vector $[V_{h,1} \dots, V_{h,M}]^T$, with a block diagonal matrix of coefficients. As a consequence, our approach is less costly than the ‘‘Scheme’’ proposed by the authors in [10,12], where they treat in two different ways the unknown u_n . Concerning the partitioned symplectic approach, the variable u_n is always explicitly approximated and the unknown v_n is discretized in an implicit way. It follows that the scheme provides stable results with larger spatial and temporal stepsizes.

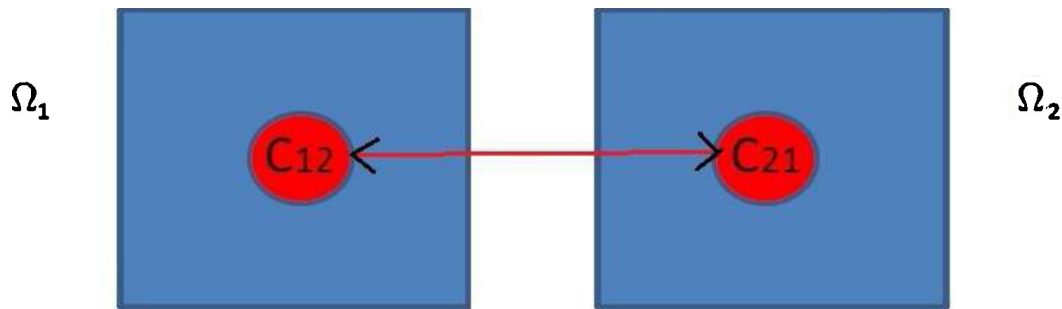


Fig. 4. An illustration of the two-patches 2D metapopulation model with fixed corridor entrance as considered in [11].

Similar arguments may be extended to the case of the second order IMSP methods; however, for the following numerical synchronization analysis we limit ourselves to applying the first order scheme to the test cases provided in [11].

4. Synchronization in a two-patches metapopulation model

An interesting topic in studying metapopulation dynamics, as pointed out in [17], is the study of the synchrony in the behaviour of the subpopulations of different patches when a coupling is imposed to the dynamics via migration. It is known that synchronous fluctuations in subpopulations increase the risk of extinction of the entire metapopulation through generating temporally correlated extinction events that may negatively affect any local rescue action. There is a tradeoff between positive and negative effects of the migration: a metapopulation whose local populations are too connected risks extinction because of synchrony, while a metapopulation whose populations are too isolated risks extinction because of low inter-patch migration rates.

In the classical metapopulation approach the models are spatially implicit in that they are described by ordinary differential equations. In [14] Jansen focuses on a predator–prey LM model while in [15] he describes the local interaction between predator and prey by RM model in which the prey population grows logistically and the predator has an Holling's type II functional response. The metapopulation consists of two populations living in two patches which are coupled by a migration which is limited only to the prey movement. The main question addressed is when synchronous and asynchronous dynamics arise: Jansen found that for very small and very large migration rates the oscillations always synchronize, while for intermediate migration rates asynchronous dynamics may arise. However, in recent years, the consideration of spatial processes in ecological systems is growing and spatially explicit modeling described by partial differential equations appears more effective for the ecological understanding of such phenomena [5,8,27,28,30]. The first metapopulation models which couple, via migration, reaction-diffusion partial differential equations in a patchy domain is provided in [11]. The authors numerically analyzed the case of a two-patch metapopulation model evolving in two-dimensional squares according to RM model dynamics, by employing the Euler IMEX finite difference scheme (implicit for the diffusion term and explicit for the reaction term). The authors assumed that the migration was restricted in both patches to a circle of fixed size radius, located in the middle of the square domains (see Fig. 4).

Because of the artificial nature of the zero-flux boundary conditions, the authors conclusions are related to transient dynamics since boundary conditions artificially pollute the solution. They found that the migration between two patches may be a new way of generating periodic plane wave phenomena (travelling waves) in natural populations modelled by oscillatory reaction-diffusion systems. Here we investigate the numerical solution of (9) ($m = 2, M = 2$) evolving in two circular domains $\Omega_i = x^2 + y^2 < \rho_{\Omega_i}^2$ with radius $\rho_{\Omega_i} = 150$, with $i = 1, 2$. The experiments were performed by modifying the two-dimensional MATLAB codes made freely available from the web site: <http://www.uoguelph.ca/mgarvie/>. Therein the discretization in space is based on a Galerkin finite-element method (see [2], [3]) with piecewise linear basis functions using a mesh generated with a MATLAB function `mesh2d`. In our experiments, we used an unstructured triangular mesh with initial edge length $h = 1/2$, obtained in Matlab with the function `distmesh` [23]. Such function optimizes the node locations by a force-based smoothing procedure and provides well-shaped meshes. Concerning the discretization in time, the linear systems are solved using MATLAB's built in function `gmres` with time step

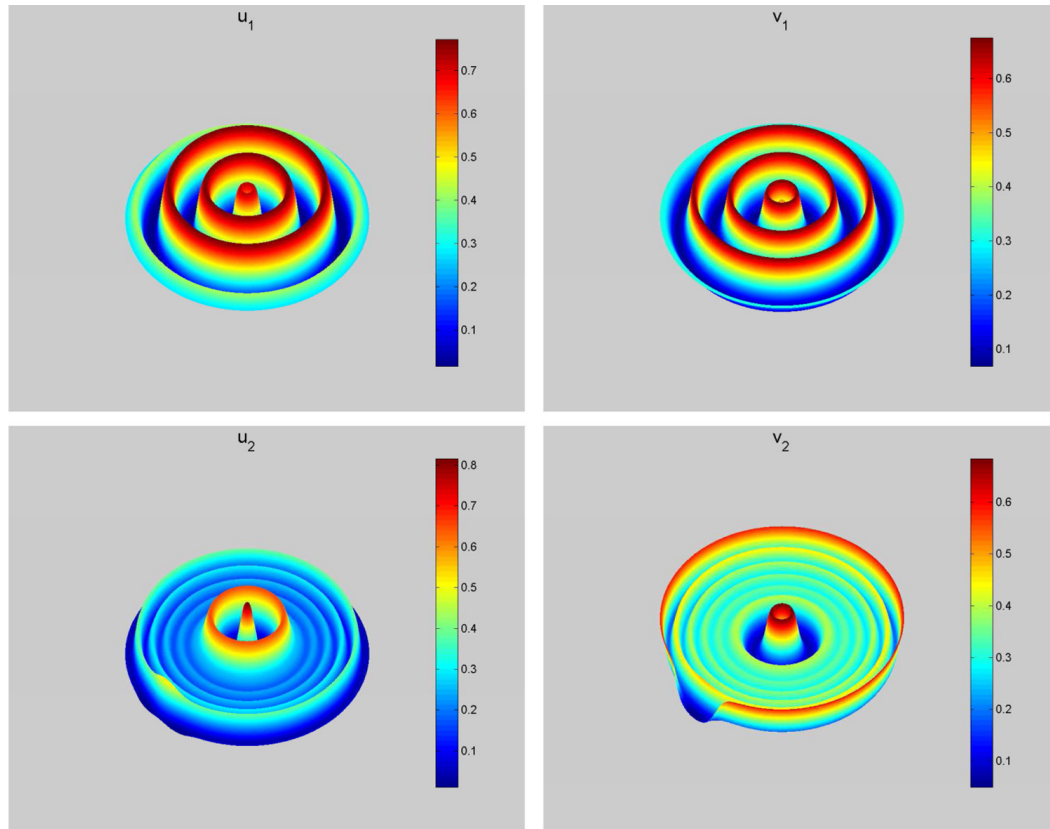


Fig. 5. An illustration of the two-patches two-dimensional metapopulation model with fixed corridor entrance. Parameter values in both patches: $l_i = 1/5$, $\chi_i = 1$, $r_i = 1$, $k_i = 1$, $c_i = 1$, $\gamma_i = 1/2$, ($i = 1, 2$), $\epsilon^{(u)} = \epsilon^{(v)} = 1$. Initial data: $u_{1,0} = 0.2$, $v_{1,0} = 0.32$, $u_{2,0} = 0.2$, $v_{2,0} = 0$. Migration rates $d_{12}^{(u)} = 0$, $d_{12}^{(v)} = 1$. First row: prey and predator within patch 1 at $T=250$. Second row: patch 2, $T=140$.

$h_T = 1/384$. The code employs the sparse matrix facilities of MATLAB when solving the linear systems which provide advantages in both matrix storage and computation time.

In the first set of experiments we fix the radius ρ_C of a circular corridor; in the second set of tests we vary the radius in order to know how such a change affects the results with respect the synchronization.

4.1. Corridors with constant radius

In the first set of experiments the length of the radius is set at $\rho_C = 5$. The initial data are the stationary states of predators and preys in Ω_1 and the stationary state of preys in Ω_2 with local extinction of predators. We assume that only predators can migrate. Our results show how predators have the ability to recolonize a patch where their species was extinct. Indeed in Fig. 5 we observe a rapid recolonization through the spreading of periodic traveling waves behind the wavefront. Notice that the wavefront speed is faster in domain Ω_2 than in Ω_1 . When we repeat the same test for $d_{12}^{(v)} = 1 \times 10^{-6}$, unlike what was reported in [11], we do not observe the generation of any new dynamics in Ω_2 without the simultaneous generation of a new dynamics in Ω_1 . The different results provided by the two first order schemes may suggest a more stable behaviour of our proposed IMSP scheme with respect to the Euler IMEX scheme.

In the second set of experiments (see Fig. 6) we assume that both predators and preys can migrate: as before, our results show the spread of periodic traveling waves behind the wavefront. This time, the wavefront speed is faster in domain Ω_1 than in Ω_2 . As for the first experiment, when we repeat the same test for lower values of migration rates, our results confirm those provided by the Euler IMEX scheme: in the long run, the generation of any new dynamics in Ω_2 always induces new dynamics in Ω_1 .

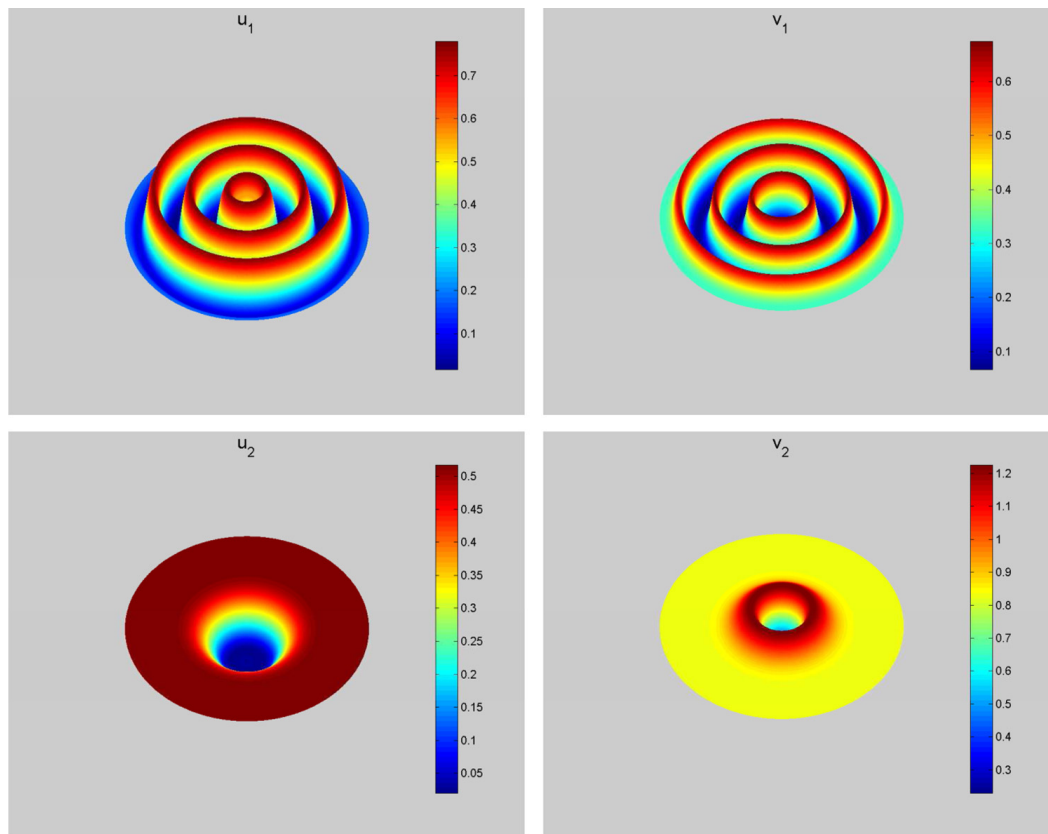


Fig. 6. Parameter values in both patches: $l_1 = 1/5, l_2 = 2/5, \chi_1 = 1, \chi_2 = 2, r_i = 1, k_i = 1, c_i = 1, \gamma_i = 1/2, (i = 1, 2), \epsilon^{(u)} = \epsilon^{(v)} = 1$. Initial data: $u_{1,0} = 0.2, v_{1,0} = 0.32, u_{2,0} = 0.1714, v_{2,0} = 0.4735$. Migration rates $d_{12}^{(u)} = d_{12}^{(v)} = 1$. First row: prey and predator within patch 1 at $T = 250$. Second row: patch 2, $T = 350$.

4.2. Variable radius corridors

We define the cross-correlation between two time series $X_i = X_i(t), i = 1, 2$

$$C(X_1, X_2) = \frac{(X_1 - \mu_1)^T (X_2 - \mu_2)}{\|X_1 - \mu_1\|_2 \|X_2 - \mu_2\|_2} \quad (11)$$

where μ_i represent the mean of the signal X_i .

The cross-correlation values range from 1 for perfectly synchronized signals to -1 for anti-correlated signals. Values close to zero denote the absence of synchronization. We are concerned here with the synchronization of the prey (predator) densities in both patches due to the coupling induced through migration. In our notation the signal $X_i(t), i = 1, 2$ represents the prey (predator) density in a given point of the domain Ω_i , as measured through time. Each pair of signals to be compared is taken in corresponding points of the two domains. We then explore the effect of the migration, both in and outside the corridor, by calculating the cross-correlation of the signals measured in several points located along the radius of each domain, at distance ρ from the center.

We expect that the signals correlate in the part of the domain occupied by the corridor and that the preys and predators synchronize therein. In Fig. 7 we show the results for both preys and predators and for different sizes of the corridor, i.e. $\rho_C = 10, 50, 100, 150$. The initial edge length of the spatial mesh has been set to $h = 1$ while the time step is $h_T = 0.1$. All the remaining parameters have been chosen as in Fig. 5, with $T = 140$. As can be appreciated, the signals are fully synchronized inside the corridor for any given corridor size, because of the migration terms which introduce a coupling of the equations for the two domains throughout the region occupied by the corridor. The migration also has an effect in the external region, but the correlation decreases with the distance from the border of the corridor. From several numerical experiments, not shown here, we noticed that the extent of the synchronization outside the corridor

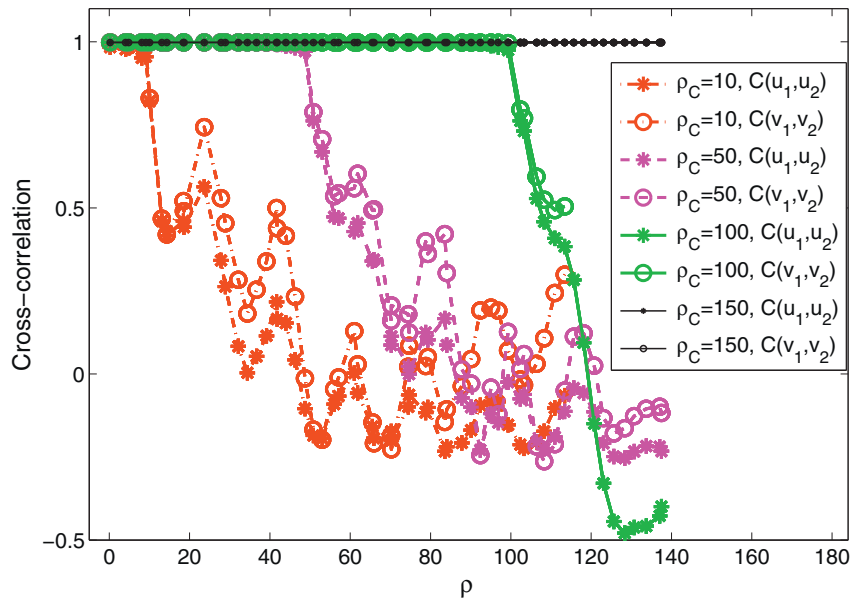


Fig. 7. Cross-correlation of prey (predator) densities in the two patches at increasing distance ρ from the domain center for different corridor radii ρ_C .

increases with time, because of the diffusion term. We might conclude that there is a time lapse separating the spread of the solution in the whole domain and the onset of the phase lock in the peripheral region.

5. Conclusions

The numerical approximation of spatially explicit models described by reaction-diffusion partial differential equations for the study of predator–prey population dynamics was performed by means of implicit-symplectic (IMSP) schemes. The performance of these schemes has been numerically evaluated on two examples of spatially explicit cyclic populations and one example of metapopulation model. The results confirm a better qualitative behaviour of the approximated solution obtained with the proposed implicit-symplectic approach in contrast with the results provided by the classical implicit–explicit schemes. The effect of the variation of the corridor size on the subpopulation dynamics synchronization has been also investigated. As expected the dynamics are fully synchronized in the corridor, while the extent of the synchronization outside the corridor increases with time, due to the diffusion term.

Acknowledgments

We thank the anonymous reviewers for their helpful comments that contributed to improve our paper. We thank also Nicholas Tavalion for having carefully read the paper and for his help in improving its revision. This work has received funding from the European Union's Seventh Framework Programme FP7 /2007–2013, SPA. 2010.1.1-04: “Stimulating the development of GMES services in specific area”, under grant agreement 263435, project title: BIODiversity Multi-Source Monitoring System: from Space To Species (BIOSOS) coordinated by CNR-ISSIA, Bari-Italy (<http://www.biosos.eu>).

References

- [1] U.M. Ascher, S.J. Ruuth, R.J. Spiteri, Implicit–explicit Runge–Kutta methods for time-dependent partial differential equations, *Applied Numerical Mathematics* 25 (1997) 151–167.
- [2] S. Brenner, L. Scott, *The Mathematical Theory of Finite Element Methods*. Vol. 15: Texts in Applied Mathematics, Springer, New York, 1994.
- [3] P. Ciarlet, *The Finite Element Method for Elliptic Problems*. Vol. 4: Studies in Mathematics and its Applications, North-Holland, Amsterdam, 1979.
- [4] C. Cosner, Variability, vagueness and comparison methods for ecological models, *Bulletin of Mathematical Biology* 58 (2) (1996) 207–246.

- [5] M.J. Conroy, Y. Cohen, F.C. James, Y.G. Matsinos, B.A. Maurer, Parameter-estimation, reliability, and model improvement for spatially explicit models of animal populations, *Ecological Applications* 5 (1995) 17–19.
- [6] F. Diele, C. Marangi, Explicit symplectic partitioned Runge–Kutta–Nystrom methods for non-autonomous dynamics, *Applied Numerical Mathematics* 61 (2011) 832–843.
- [7] F. Diele, C. Marangi, S. Ragni, Implicit – symplectic partitioned (IMSP) Runge–Kutta schemes for predator–prey dynamics, *AIP Conference Proceedings* 1479 (2012) 1177–1180.
- [8] J.B. Dunning, D.J. Stewart, B.J. Danielson, B.R. Noon, T.L. Root, R.H. Lamberson, E.E. Stevens, Spatially explicit population models – current forms and future uses, *Ecological Applications* 5 (1995) 3–11.
- [9] J. Enright, Climate and population regulation. The biogeographer’s dilemma, *Oecologia* 24 (4) (1976) 295–310.
- [10] M.R. Garvie, Finite-difference schemes for reaction-diffusion equations modeling predator–prey interactions in MATLAB, *Bulletin of Mathematical Biology* 69 (2007) 931–956.
- [11] M.R. Garvie, M. Golinski, Metapopulation dynamics for spatially extended predator–prey interactions, *Ecological Complexity* 7 (2010) 55–59.
- [12] M.R. Garvie, C. Trenchea, Finite element approximation of spatially extended predator–prey interactions with the Holling type II functional response, *Numerische Mathematik* 107 (4) (2012) 641–667.
- [13] E. Hairer, C. Lubich, G. Wanner, *Geometric Numerical Integration. Structure-Preserving Algorithms for Ordinary Differential Equations*, Springer-Verlag, Berlin, 2002.
- [14] V.A.A. Jansen, Regulation of predator–prey systems through spatial interactions: a possible solution to the paradox on enrichment, *Oikos* 74 (1995) 384–390.
- [15] V.A.A. Jansen, The dynamics of two diffusively coupled predator–prey populations, *Theoretical Population Biology* 59 (2001) 119–131.
- [16] R. Levins, Some demographic and genetic consequences of environmental heterogeneity for biological control, *Bulletin of the Entomological Society of America* 15 (1969) 237–240.
- [17] K. Koelle, J. Vandermeer, Dispersal-induced desynchronization: from metapopulations to metacommunities, *Ecology Letters* 8 (2005) 167–175.
- [18] T. Koto, IMEX Runge Kutta schemes for reaction diffusion equations, *Journal of Computational and Applied Mathematics* 215 (2008) 182–195.
- [19] E. Latos, T. Suzuki, Y. Yamada, Transient and asymptotic dynamics of a prey–predator system with diffusion, *Mathematical Methods in the Applied Sciences* 35 (2012) 1101–1109.
- [20] R. May, *Stability and Complexity in Model Ecosystems*, Princeton University Press, Princeton, 1974.
- [21] R.I. McLachlan, On the numerical integration of ordinary differential equations by symmetric composition methods, *SIAM Journal on Scientific Computing* 16 (1995) 151–168.
- [22] A.B. Medvinsky, S.V. Petrovskii, I.A. Tikhonova, H. Malchow, B.-L. Li, Spatiotemporal complexity of plankton and fish dynamics, *SIAM Review* 44 (3) (2002) 311–370.
- [23] P.O. Persson, G. Strang, A simple mesh generator in MATLAB, *SIAM Review* 46 (2) (2004) 329–345.
- [24] A. Okubo, S.A. Levin, *Diffusion and Ecological Problems: Modern Perspectives*, Springer, New York, 2001.
- [25] M. Rosenzweig, R. MacArthur, Graphical representation and stability conditions of predator–prey interactions, *The American Naturalist* 97 (1963) 209–223.
- [26] J.A. Sherratt, M.J. Smith, Periodic travelling waves in cyclic populations: field studies and reaction-diffusion models, *Journal of the Royal Society Interface* 5 (2008) 483–505.
- [27] A. South, Dispersal in spatially explicit populations models, *Conservation Biology* 13 (1999) 1039–1046.
- [28] S. Strohm, R. Tyson, The effect of habitat fragmentation on cyclic population dynamics: a numerical study, *Bulletin of Mathematical Biology* 71 (2001) 1323–1348.
- [29] P. Turchin, G. Batzli, Availability of food and the population dynamics of arvicoline rodents, *Ecology* 82 (2001) 1521–1534.
- [30] M.G. Turner, G.J. Arthaud, R.T. Engstrom, S.J. Hejl, J.G. Liu, S. Loeb, K. McKelvey, Usefulness of spatially explicit population models in land management, *Ecological Applications* 5 (1995) 12–16.